

A PERIOD-PROJECTION FACTOR RELATION FOR CEPHEIDS

Nardetto, N.¹, Mourard, D.², Mathias, Ph.², Fokin, A.³ and Gillet, D.⁴

Abstract. The projection factor is a key quantity for the interferometric Baade-Wesselink (hereafter IBW) and surface-brightness (hereafter SB) methods of determining the distance of Cepheids. We aim to determine consistent projection factors that include the dynamical structure of the Cepheids' atmosphere. Hydrodynamical models of δ Cep and ℓ Car have been used to validate a spectroscopic method of determining the projection factor. This method, based on the amplitude of the radial velocity curve, is applied to eight stars observed with the HARPS spectrometer. The projection factor is divided into three sub-concepts : (1) a geometrical effect, (2) the velocity gradient within the atmosphere, and (3) the relative motion of the "optical" pulsating photosphere compared to the corresponding mass elements (hereafter f_{o-g}). Both, (1) and (3) are deduced from geometrical and hydrodynamical models, respectively, while (2) is derived directly from observations. The Fe I 4896.439 Å line is found to be the best one to use in the context of IBW and SB methods. A coherent and consistent period-projection factor relation (hereafter Pp relation) is derived for this specific spectral line: $p = [-0.064 \pm 0.020] \log P + [1.376 \pm 0.023]$. This procedure is then extended to derive dynamic projection factors for any spectral line of any Cepheid. This Pp relation is an important tool for removing bias in the calibration of the period-luminosity relation of Cepheids.

1 Introduction : the interferometric Baade-Wesselink Method

Long-baseline interferometers currently provide a new, quasi-geometric way to calibrate the Cepheids period-luminosity relation. Indeed, it is now possible to determine the distance of galactic Cepheids up to 1kpc with the interferometric Baade-Wesselink method, hereafter IBW method. Interferometric measurements lead to angular diameter estimations over the whole pulsation period, while the stellar radius variations can be deduced from the integration of the pulsation velocity. The latter is linked to the observational velocity deduced from spectral line profiles by the projection factor p . In this method, angular and linear diameters have to correspond to the same physical layer in the star to correctly estimate the distance (Nardetto et al. 2004). We propose a division of the projection factor into sub-concepts in order to allow a direct constraint from HARPS spectroscopic observations of eight stars : R Tra, S Cru, Y Sgr, β Dor, ζ Gem, RZ Vel, ℓ Car, RS Pup, with periods ranging from 4.7 to 42.9 days. More detail can be found in Nardetto et al. 2007 (hereafter Paper I).

2 Decomposition of the projection factor

First of all, we have to provide a definition for the projection factor that should be applied in the IBW and SB methods. We define the interferometric projection factor as

$$p = \frac{\Delta V_p^o}{\Delta R V_c} \quad (2.1)$$

where ΔV_p^o is the amplitude of the pulsation velocity curve associated to the photosphere (subscript p) of the star. It corresponds exactly to the *optical* (subscript o) barycenter of the photosphere defined by $\tau_c = 2/3$,

¹ Max-Planck-Institut für Radioastronomie, Auf dem Hügel 69, 53121 Bonn, Germany

² Observatoire de la Côte d'Azur, Dpt. Gemini, UMR 6203, F-06130 Grasse, France

³ Institute of Astronomy of the Russian Academy of Sciences, 48 Pjatnitskaya Str., Moscow 109017 Russia

⁴ Observatoire de Haute Provence, 04870 Saint-Michel l'Observatoire, France

where τ_c is the optical depth in the continuum. ΔRV_c is the amplitude of the radial velocity curve obtained with the centroid method, i.e. the first moment of the spectral line. This is required for obtaining a projection factor independent of the rotation of the star and the natural width of the spectral lines (see Fig. 8, Nardetto et al. 2006a). We insist on this definition of the radial velocity since it is absolutely required to allow important comparisons between the projection factors of Cepheids.

We now divide the projection factor:

$$p = p_o f_{o-g} f_{\text{grad}},$$

into different quantities where.

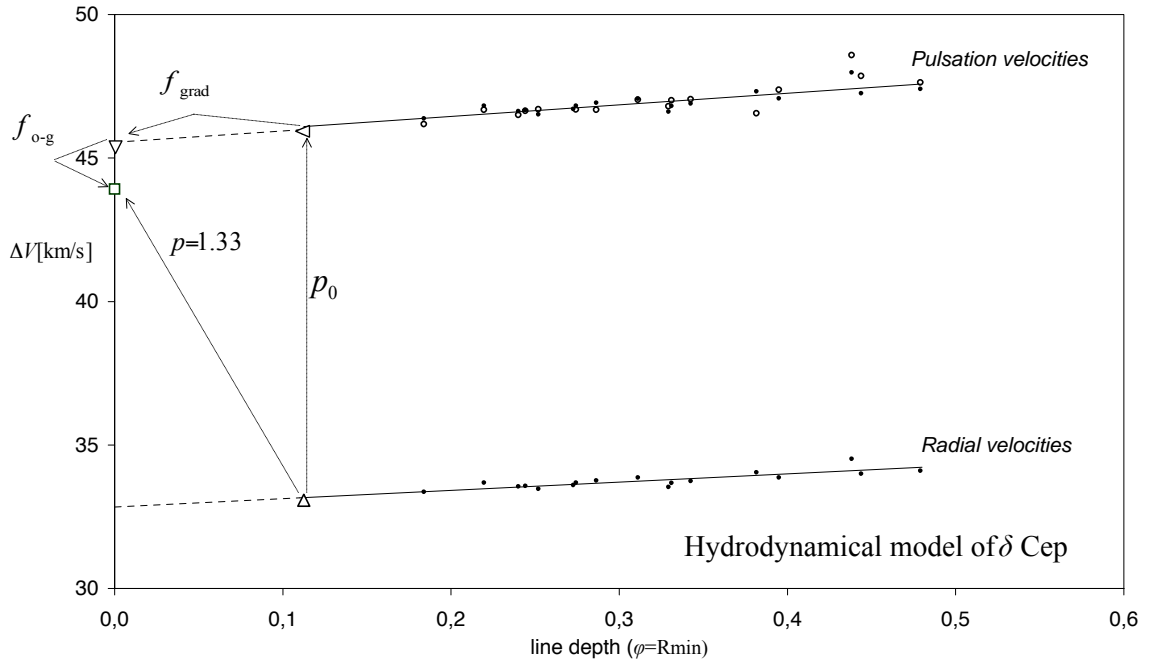


Fig. 1. The projection factor decomposition ($p = p_o f_{\text{grad}} f_{o-g}$) in the case of the Fe I 4896.439 Å spectral line: ΔRV_c (\triangle), ΔV_1^g (\diamond), ΔV_p^g (triangle down) and ΔV_p^o (Box). The Reference value $p = 1.33$ is indicated. The proposed method of the f_{grad} determination is to first derive ΔRV_c as a function of the line depth for all spectral lines (lower part, black points). This relation is defined as $\Delta RV_c = a_0 D + b_0$. Then, when translating $(D, \Delta RV_c)$ points into $(D, p_o \Delta RV_c)$, a new linear relation is found (upper part of the figure, black points). This new relation is (1) coherent with the pulsation velocity gradient in the atmosphere (open circles) and (2) its zero-point is consistent with the pulsation velocity corresponding to the *gaseous* layer of the photosphere: ΔV_p^g (triangle down). The decomposition of the projection factor is thus self-consistent, and f_{grad} can be directly derived from observations for any spectral line using the relation : $f_{\text{grad}} = \frac{b_0}{a_0 D + b_0}$, where D is the line depth of the considered spectral line.

- $p_o = \frac{\Delta V_1^g}{\Delta RV_c}$ is the geometrical projection factor. It corresponds to an integration of the pulsation velocity field projected on the line of sight and weighted by the surface brightness of the star. To derive p_o , we consider a linear law for the continuum-intensity distribution of the star defined by $I(\cos(\theta)) = 1 - u_V + u_V \cos(\theta)$, where u_V is the limb-darkening of the star in the V band. p_o is derived for all stars. In addition, we find that a slight correction must be applied to allow a comparison between geometric and hydrodynamic modeling. The hydrodynamical models of δ Cep and ℓ Car are actually used to calibrate the Pp_o relation.

- $f_{o-g} = \frac{\Delta V_p^o}{\Delta V_p^g}$, where ΔV_p^g is the gas (subscript g) velocity associated to the *optical* barycenter ($\tau_c = 2/3$) of the photosphere. Thus, f_{o-g} is linked to the distinction between the *optical* and *gas* photospheric layers. The *optical* layer is the location where the continuum and line photons are generated (e.g. the location of the photosphere). The *gas* layer is the location of some mass element in the hydrodynamic model mesh where, at some moment in time, the photosphere is located. Given that the location of the photosphere moves through different mass elements as the star pulsates, the two “layers” have different velocities, hence the necessity of the

Table 1. Hydrodynamical models of Cepheids.

Name	P [days]	T_{eff} [K]	$\frac{L}{L_{\odot}}$	$\frac{M}{M_{\odot}}$	$\frac{\bar{R}}{R_{\odot}}$
S Cru	4.7	5900	1900	5.6	42
δ Cep	5.4	5877	1995	4.8	43
Y Sgr	5.7	5850	2200	5.0	45
β Dor	9.9	5500	3500	5.5	65
ζ Gem	10.4	5500	3600	5.0	64
RZ Vel	21.6	5400	7450	7.0	109
ℓ Car	34.4	5225	21000	11.5	180
RS Pup	42.9	5100	22700	9.7	186

f_{o-g} definition. Indeed, the interferometer in the continuum is only sensitive to the *optical* layer. This quantity is derived directly from the hydrodynamical models of Cepheids (see Table 1).

- $f_{grad} = \frac{\Delta V_p^g}{\Delta V_1^g}$, where ΔV_1^g is the *gas* velocity associated to the optical barycenter ($\tau_1 = 2/3$) of the line-forming (subscript l) region. Thus, f_{grad} is linked to the velocity gradient in the atmosphere of the star. This quantity is derived directly from spectroscopic observations (see next Sect.).

The consistency of the projection factor decomposition is validated by the hydrodynamical models of δ Cep and ℓ Car. The case of δ Cep is presented on Fig. 1.

3 Is there a consistent way to derive f_{grad} directly from observations?

Let assume a linear relation between the line depth and the position of the line-forming region in the atmosphere of the star. Then, considering different spectral lines spread all over the atmosphere, it should be possible to determine the velocity gradient within the atmosphere. To test these ideas, we consider the spectral line depth corresponding to the minimum extension of the star (D in the following, see paper I). Then, we derive ΔRV_c for 17 selected spectral lines, and find a very interesting observational linear correlation $\Delta RV_c = a_0 D + b_0$ for all stars of our sample (see Fig. 2 and Table 2). Following the projection factor decomposition, we can derive f_{grad} by using the following relation : $f_{grad} = \frac{b_0}{a_0 D + b_0}$. f_{grad} depends thus on the spectral line considered. And it seems clear that a spectral line that forms close to the photosphere implies small differences (in velocity) between the line-forming region and the photosphere. We thus finally find that the Fe I 4896 Å spectral line (with D very small: 0.08 in average over all stars) is the best one to use in the context of the IBW and SB methods.

By combining all quantities (p_o , f_{grad} and f_{o-g}), we are able to derive a Pp relation for the first time. p_o and f_{o-g} are deduced from geometrical and hydrodynamical models, respectively, while f_{grad} is derived directly from observations. A summary of the results is given in Table 2 and illustrated in Fig. 3. The resulting linear law is:

$$p = [-0.064 \pm 0.020] \log P + [1.376 \pm 0.023]. \quad (3.1)$$

This relation holds only for the Fe I 4896.439 Å spectral line.

4 Discussion

The derived Pp relation will be useful in the context of the IBW and SB methods. For example, if we compare Eq. 3.1 with the usual value widely used in the community $p = 1.36$ (Burki et al. 1982), we obtain a correction for the projection factor depending on the period. It is then possible to translate it into a bias on distances and absolute magnitudes. By this process, we obtain the relation:

$$\Delta M_V = 0.10 \log P - 0.03 \quad (4.1)$$

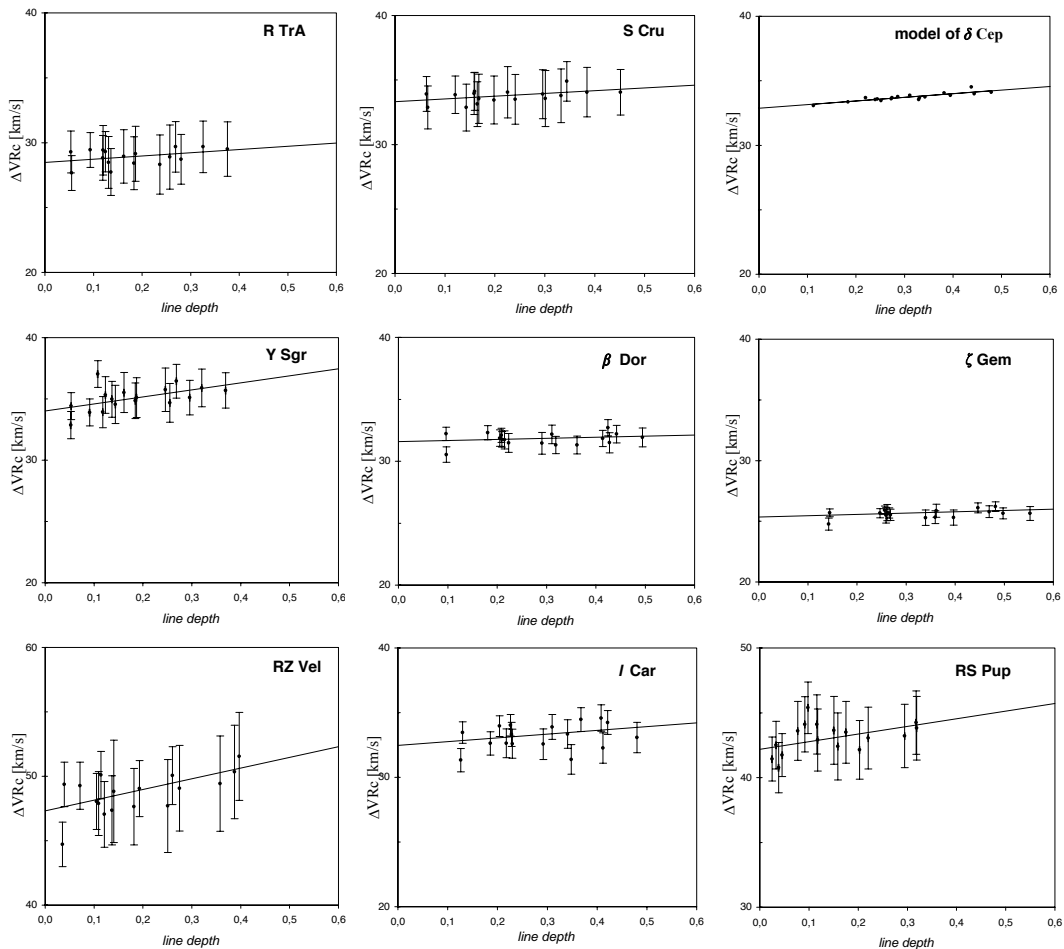


Fig. 2. ΔRV_c as a function of the depth D of the spectral line considered. Uncertainties are indicated. Stars are presented with increasing period. The δ Cep model is also indicated for comparison. Linear correlations are derived for all stars (see Table 2). The f_{grad} quantity is derived from these relations.

where ΔM_V is the correction to consider on the PL relation. We thus conclude that one can make an errors of 0.10 and 0.03 on the slope and zero-point of the PL relation, respectively, if $p = 1.36$ is used for all stars instead of the Pp relation. This correction is, however, only indicative because it is indeed restricted to our definition of the projection factor (Eq. 2.1) and to the Fe I 4896.439 Å spectral line.

It is now possible to refine the IBW and SB methods. First, we suggest using the RV_c radial velocity to avoid bias related to the rotation velocity of the star (even if Cepheids are supposed to be slow rotators) and the width of the spectral line. One then has to determine the RV_c curve and force the average to be zero in order to avoid γ -velocity effects. Due to our careful definition of p , the projection factors proposed in this paper are indeed independent of the γ -velocity. The spectral line considered must have a depth lower than 0.1 and should be the same for all considered Cepheids. The low depth of the spectral line is required to diminish the impact of the velocity gradient. If the Fe I 4896.439 Å is used, one can use Eq. 3.1 directly to determine the dynamic projection factors of Cepheids. If not, we propose the following method. Given the line depth of the spectral line considered for each Cepheid, it is possible to determine the f_{grad} from a_0 and b_0 (Table 2). If the Cepheid being studied is not in our sample, Fig. 2 of Paper I can be used. Then p_o can be determined using a geometrical model. However, the consistency (at a level lower than 0.025 on p) between interferometric observations, geometrical, and hydrodynamical models should be studied in detail in the future. For f_{o-g} , one can use:

$$f_{o-g} = [-0.023 \pm 0.005] \log P + [0.979 \pm 0.005], \quad (4.2)$$

Table 2. Derived projections factors for all stars computed from the decomposition presented in Eq. 2.2.

Name	HD	P ^(b) [days]	a_0 ^(c)	b_0 ^(c)	p_o ^(d)	f_{grad} ^(e)	f_{o-g} ^(f)	p ^(g)
R TrA	135592	3.38925	$2.50_{\pm 4.55}$	$28.48_{\pm 0.90}$	$1.396_{\pm 0.010}$	$0.995_{\pm 0.009}$	$0.967_{\pm 0.005}$	$1.34_{\pm 0.03}$
S Cru	112044	4.68976	$2.13_{\pm 3.61}$	$33.33_{\pm 0.90}$	$1.392_{\pm 0.010}$	$0.996_{\pm 0.007}$	$0.966_{\pm 0.005}$	$1.34_{\pm 0.03}$
Y Sgr	168608	5.77338	$5.76_{\pm 3.53}$	$34.01_{\pm 0.12}$	$1.387_{\pm 0.010}$	$0.991_{\pm 0.005}$	$0.962_{\pm 0.005}$	$1.32_{\pm 0.02}$
β Dor	37350	9.84262	$0.86_{\pm 1.31}$	$31.59_{\pm 0.40}$	$1.380_{\pm 0.010}$	$0.997_{\pm 0.004}$	$0.955_{\pm 0.005}$	$1.31_{\pm 0.02}$
ζ Gem	52973	10.14960	$1.09_{\pm 0.89}$	$25.35_{\pm 0.31}$	$1.380_{\pm 0.010}$	$0.994_{\pm 0.005}$	$0.953_{\pm 0.005}$	$1.31_{\pm 0.02}$
RZ Vel	73502	20.40020	$8.32_{\pm 5.95}$	$47.31_{\pm 1.02}$	$1.375_{\pm 0.010}$	$0.994_{\pm 0.004}$	$0.951_{\pm 0.005}$	$1.30_{\pm 0.02}$
ℓ Car	84810	35.55134	$2.89_{\pm 2.26}$	$32.48_{\pm 0.67}$	$1.366_{\pm 0.010}$	$0.989_{\pm 0.005}$	$0.944_{\pm 0.005}$	$1.27_{\pm 0.02}$
RS Pup	68860	41.51500	$5.89_{\pm 5.58}$	$42.19_{\pm 0.88}$	$1.360_{\pm 0.010}$	$0.995_{\pm 0.005}$	$0.943_{\pm 0.005}$	$1.28_{\pm 0.02}$
δ Cep ^(a)	213306	5.419	2.90	32.84	$1.390_{\pm 0.010}$	$0.990_{\pm 0.005}$	$0.963_{\pm 0.005}$	$1.33_{\pm 0.02}$
ℓ Car ^(a)	84810	35.60	5.20	37.02	$1.366_{\pm 0.010}$	$0.988_{\pm 0.005}$	$0.944_{\pm 0.005}$	$1.27_{\pm 0.02}$

^a δ Cep and ℓ Car are hydrodynamical models

^b The corresponding Julian dates (T_o) can be found in Nardetto et al. 2006a.

^c Linear relations (Fig 2) between the amplitude of the velocity curves and the line depth (at minimum extension of the star), $\Delta RV_c = a_0 D + b_0$ for all stars, together with the 1σ uncertainty.

^d p_o is derived from the linear limb-darkening laws of Claret et al. (2000) based on the static models of Kurucz (1992). We then apply a slight correction based on the δ Cep and ℓ Car hydrodynamical models: $p_o[\text{hydro}] = p_o[\text{geo}] - (0.0174 \log P - 0.0022)$ to take the dynamical structure of the Cepheid's atmosphere into account.

^e f_{grad} is derived directly from observations using Eq. $f_{\text{grad}} = \frac{b_0}{a_0 D + b_0}$. It is important to notice that the results indicated here correspond to the Fe I 4896.439 Å line. In the case of a modeled star, it is derived directly from the hydrodynamical model.

^f f_{o-g} is derived directly from the hydrodynamical models.

^g p -factors defined by $p = p_o f_{\text{grad}} f_{o-g}$. p_o and f_{o-g} are derived from geometrical and hydrodynamical models respectively. f_{grad} is derived from observations.

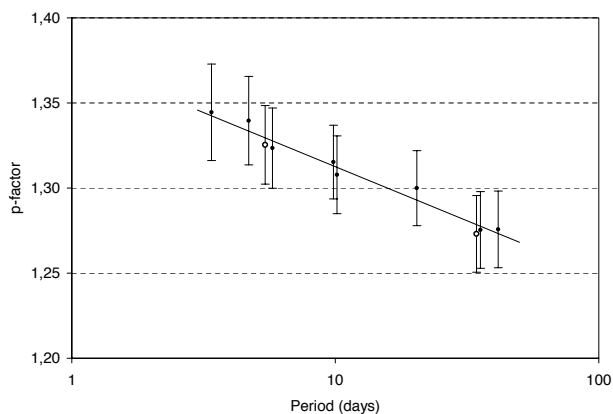


Fig. 3. The projection factor ($p = p_o f_{\text{grad}} f_{o-g}$) as a function of the logarithm of the period. Black points and open circles correspond to observations and models.

even if this relation has to be confirmed observationally in the future. Finally, the projection factor of Cepheids, following our decomposition, is $p = p_o f_{\text{grad}} f_{o-g}$. This procedure should be applied to avoid bias in the calibration of the PL relation.

However, we know that the masking cross-correlation method is widely used to increase the signal-to-noise

ratio on radial velocity measurements. In that case however, one cannot exclude the impact of the rotation, the spectral lines' width, and γ -velocities effects. Nevertheless, we can still provide a Pp relation that is more appropriate considering an average line depth of $D = 0.25$. We find $p = [-0.075 \pm 0.031] \log P + [1.366 \pm 0.036]$. Another important point is that we provide visible projection factors that should be used with visible spectroscopic observations. If one used infrared spectroscopic observations to derive the pulsation velocity, one should use specific infrared projection factors. Indeed, in the infrared, the limb darkening is supposed to be lower and the corresponding p_o -factors higher (certainly about 4%). But, spectral lines also form higher in the atmosphere (i.e. in the upper part of the atmosphere), which supposes a lower f_{grad} . More studies have to be carried out to derive an infrared Pp relation.

The next step is now to provide a remarkable insight into the dynamical structure of Cepheids' atmosphere by investigating, based on models of new generation, the relation presented in Nardetto et al. (2006a) between the pulsating period and the spectral lines asymmetry curves (hereafter PA relation). Important links should be indeed found between the line asymmetry and f_{o-g} . However, right now, *no model is able to reproduce this PA relation in a satisfactory way*. For that purpose, it seems required to dramatically increase the refinement of hydrodynamical models, including convective energy transport, adaptive mesh, and a careful description of the radiative transfer. We also expect in a near future important spectro-interferometric observations with high spectral resolution (see e.g. the VEGA project with $R \simeq 30000$, Mourard et al. 2007 and Stee et al. 2007). Then, it would be interesting with such strong observational constraints (spectral line asymmetry and high-angular resolution) to test the consistency of the models. In particular, it seems conceivable to constrain the parameters of the 1D or multi-D convection. In that context, such models of new generation will be crucial for our understandings of physical processes involved in the dynamics of Cepheids' atmosphere.

Another limiting aspect concerns the limb-darkening. Computation of limb-darkening profiles at different wavelengths and pulsational phases is needed in the IBW method not only to derive the interferometric angular diameters, but also to determine the geometric projection factor. However, theoretical results concerning limb-darkening are currently inconsistent at an important level (see for example Marengo et al. 2003, Fig. 3, and Nardetto et al. 2006b, Fig. 3). On the observation point of view, it should be possible in a near future to constrain this physical quantity directly from interferometric observations in the continuum (see for e.g. Aufdenberg et al. 2003). However, it is likely that new models including a refined description of the radiative transfer (NLTE, spherical geometry) within the pulsating envelope will be certainly required to reproduce the observational wavelength and phase-dependence of the limb-darkening.

5 Conclusion

This Pp relation is an important tool for removing bias in the calibration of the period-luminosity relation. We emphasize that, if a constant projection factor is used to constrain the PL relation, an error of 0.10 and 0.03 magnitudes can be done, respectively, on the slope and zero-point of the PL relation. This can even be much more if the wrong definition of the radial velocity is used. The intercept of this relation is confirmed by recent HST observations, while the slope should be constrained in a near future by surface-brightness distances of LMC Cepheids (Fouqué et al. 2007, submitted to A&A).

References

- Aufdenberg, J. P., Hauschildt, P. H., Baron, E., 2003, ASPC, 288, 239A
- Fouqué, P., Arriagada, P., Storm, J., et al. 2007, A&A, submitted.
- Marengo, M., Karovska, M., Sasselov, D. D., et al. 2003, ApJ, 589, 975
- Mourard, D., Bonneau, D., Clausse, J.-M., et al. 2006, SPIE, 6268E, 118M
- Nardetto, N., Fokin, A., Mourard, D., et al. 2004, A&A, 428, 131
- Nardetto, N., Mourard, D., Kervella, P., et al. 2006a, A&A 453, 309
- Nardetto, N., Fokin, A., Mourard, D., et al. 2006b, A&A, 454, 327
- Nardetto, N., Mourard, D., Mathias, P. et al. 2007, A&A, 471, 661N (paper I)
- Stee, P, Mourard, D., Daniel, B. et al. 2006, SPIE, 6268E, 119S